

SINGLE-CRYSTAL NEUTRON-DIFFRACTION STUDY OF PYROPE IN THE TEMPERATURE RANGE 30–1173 K

GILBERTO ARTIOLI¹ AND ALESSANDRO PAVESE

Dipartimento di Scienze della Terra, Università di Milano, via Botticelli 23, I-20133 Milano, Italy

KENNY STÅHL

Department of Chemistry, Technical University of Denmark, DK-2800 Lyngby, Denmark

RICHARD K. McMULLAN

Department of Chemistry, Brookhaven National Laboratory, Upton, New York 11973, U.S.A.

ABSTRACT

Single-crystal neutron-diffraction data were collected over the temperature range 30–1173 K on a pyrope crystal from the Dora Maira Massif, Western Alps, Italy. The study expands the structure analysis of synthetic end-member pyrope previously performed with X-ray single-crystal diffraction over a wide temperature range. The neutron nuclear scattering allows a more accurate definition of the atomic displacement parameters and their temperature dependence. The problems involved in the characterization of the atomic displacement parameters in garnet minerals, and especially in pyrope, have implication for the correct interpretation of the physical and thermodynamic properties of the garnet structure. The present analysis of the atomic displacement properties by the higher cumulants model in the Gram–Charlier series approximation shows that the anharmonic contribution to the dynamic part of the magnesium site displacement is significant above 700 K. No evidence is found for static site disorder in the dodecahedral Mg site by refinement with split-atom models, and the intercept at 0 K resulting from linear interpolation of the high-temperature harmonic displacement coefficients is not statistically significant. The refinement of high-order displacement-tensor components results in significantly lower figures of merit in the whole explored temperature range.

Keywords: pyrope, neutron diffraction, anharmonicity, crystal structure, Dora Maira massif, Italy.

SOMMAIRE

Des données de diffraction neutronique ont été obtenues sur un cristal unique de pyrope provenant du massif de Dora Maira, dans les Alpes Occidentales, en Italie, sur un intervalle de température entre 30 et 1173 K. Notre étude s'ajoute à l'analyse structurale antérieure d'un échantillon synthétique de pyrope par diffraction X, aussi effectuée sur un large intervalle de température. La dispersion des neutrons par les nucléi permet une définition plus précise des paramètres de déplacements atomiques et de leur dépendance sur la température. Les problèmes qu'implique la caractérisation de ces paramètres dans les minéraux du groupe du grenat, et plus particulièrement le pyrope, ont des implications pour l'interprétation correcte des propriétés physiques et thermodynamiques de la structure des grenats. Notre analyse des propriétés des déplacements atomiques par la méthode des cumulants de degré plus élevé dans l'approximation de la série de Gram–Charlier montre que la contribution anharmonique à la partie dynamique du déplacement du site du magnésium est importante à une température supérieure à 700 K. Nous ne trouvons aucune indication de désordre de position statique dans le cas du site dodécaédrique du Mg, suite à nos affinements de modèles à atomes "divisés"; l'intercepte à 0 K résultant de l'interpolation linéaire des coefficients de déplacement harmonique à température élevée n'est pas statistiquement significative. L'affinement des composantes de degré élevé des tenseurs de déplacement a donné une amélioration significative de la figure de mérite sur l'intervalle complet de température.

(Traduit par la Rédaction)

Mots-clés: pyrope, diffraction neutronique, anharmonicité, structure cristalline, massif de Dora Maira, Italie.

INTRODUCTION

A substantial amount of work has been devoted to garnet-group minerals in the past. They are important phases in high-pressure and high-temperature metamorphic and igneous assemblages, and several features of their crystal

chemistry and physical properties cast disquieting shadows upon our ability to interpret the details of the crystal structure of a garnet at a fundamental level.

Unresolved problems, for example, concern the thermodynamic properties of garnet solid-solutions (Cressey 1981, Geiger *et al.* 1987, Berman 1990, Koziol & Bohlen

¹ E-mail address: artioi@iunmix.terra.unimi.it

1992), especially along the pyrope – grossular, pyrope – almandine, almandine-spessartine, and almandine-grossular joins. The debated non-ideality of these solid solutions (Ungaretti *et al.* 1995), in particular those involving the pyrope component, could in principle depend on structural subsite disorder (Zemann 1962, Cressey 1981, Hofmeister & Chopelas 1991, Pilati *et al.* 1996), on non-harmonic vibrational behavior of the cations in the dodecahedral site (Winkler *et al.* 1991), on cation clustering at a local level (Ganguly *et al.* 1993), or on the non linear deformation of the X polyhedron (Quartieri *et al.* 1995). It is remarkable that most authors fail to reproduce and interpret in detail the experimental observations in some garnet end-members, pyrope and almandine in particular. The problems concern either the anomalously high heat capacity observed at low temperature (Kieffer 1980, Haselton & Westrum 1980, Hofmeister & Chopelas 1991), or the anomalously large atomic displacement parameters of the Mg and Fe cations observed by diffraction methods, and not reproducible by simulations of lattice dynamics (Patel *et al.* 1991, Winkler *et al.* 1991, Pilati *et al.* 1996).

The crystal structure of pyrope ($Mg_3Al_2Si_3O_{12}$, *Ia3d*, $Z=8$) has been thoroughly investigated by X-ray diffraction (Zemann & Zemann 1961, Gibbs & Smith 1965, Meagher 1975, Armbruster *et al.* 1992, Armbruster & Geiger 1993, Sawada 1993) and FTIR spectroscopy (Geiger *et al.* 1992). All structural studies performed at low or high temperature failed to reveal any evidence of subsite Mg disorder, but instead indicate large anisotropy of the Mg harmonic vibration. The recent study of Pavese *et al.* (1995) considerably extended the temperature range investigated with single-crystal X-ray diffraction, and the findings support these conclusions. Furthermore, it presents evidence of weak anharmonic vibrational effects of the Mg cation at high temperature. Most authors now seem to agree on the "dynamic" nature of the disorder of the Mg atom in pyrope, though there still are claims that a model based on statistical subsite disorder can adequately explain the anomalous experimental features observed (Pilati *et al.* 1996).

We have undertaken a single-crystal neutron-diffraction study of pyrope over a wide temperature range, in an attempt to obtain solid experimental evidence for the postulated anharmonic behavior of Mg in pyrope. In addition, this study is intended to characterize the dependencies of displacements of the nuclei on temperature as a means of distinguishing between static and dynamic disorder of atoms in the structure.

SAMPLE

Available neutron beams are much weaker than X-ray beam fluxes available at laboratory or advanced sources, in terms of total flux at the sample. It is therefore necessary to perform diffraction experiments at reactors or pulsed neutron sources with relatively large single crystals. Crystals of synthetic pyrope cannot be grown with volumes larger than 0.1 mm³ at present. This is about one

order of magnitude less than the minimum single-crystal volume useful for neutron diffraction from anhydrous compounds. We therefore had to rely on large natural single crystals of pyrope. The Dora Maira pyrope (Chopin 1984, Schertl *et al.* 1991), which occurs as megablasts in high-grade blueschist rocks, is the only reported occurrence of pyrope with a small amount of almandine and grossular as solid-solution components. The megablasts, up to 10–20 cm in size, are composed of a pyrope matrix containing abundant inclusions of other mineral phases, mainly muscovite, staurolite, and kyanite.

Prior to data collection, thick slides of the composite megablasts were checked for crystal quality using texture analysis on a Huber 5-circle powder diffractometer. Details of the texture analysis have been reported previously (Amisano Canesi *et al.* 1994). A crystal of 2.83 × 2.87 × 3.02 mm³ was finally extracted from the center of a slab cut through the megablasts.

Electron-probe micro-analysis on different areas of the pyrope matrix close to the region of crystal extraction resulted in the formula $(Mg_{0.92}Fe_{0.05}Ca_{0.03})Al_2Si_3O_{12}$, and indicated a remarkable chemical homogeneity of the matrix crystal.

EXPERIMENTAL

Collection of neutron-diffraction data

Neutron-diffraction intensity data were collected at 30, 100 and 293 K at the Neutron Research Laboratory, Studsvik, Sweden, and at 295, 773, 973, and 1173 K at the High Flux Beam Reactor, Brookhaven National Laboratory, Brookhaven, New York; the same crystal was used for all experiments.

The required low temperature was obtained using a CTI Cryogenics two-step closed-cycle He cooler, installed

TABLE 1. EXPERIMENTAL PARAMETERS FOR COLLECTION OF SINGLE-CRYSTAL NEUTRON-DIFFRACTION DATA AT VARIOUS TEMPERATURES AND DETAILS OF REFINEMENT

T (K)	30	100	293*	295*	295**	773	973	1173
monochr.	Ca(220)	Cu(220)	Cu(220)	Be(002)	Be(002)	Be(002)	Be(002)	Be(002)
λ (Å)	1.2150	1.2150	1.2150	1.0462	1.0462	1.0462	1.0462	1.0462
cell a (Å)	11.441	11.442	11.450	11.455	11.457	11.512	11.536	11.559
scan mode	ω -2 θ	ω -2 θ	ω -2 θ	ω -2 θ	ω -2 θ	ω -2 θ	ω -2 θ	ω -2 θ
scan angle	2.5° \clubsuit	2.0° \clubsuit	2.5° \clubsuit	1.555 + 3.0° \clubsuit	1.555 + 2.855tg θ			
max. (sin θ / λ)	0.79	0.79	0.79	0.88	0.88	0.88	0.88	0.88
meas. refl.	584	609	610	1435	1301	832	840	848
indep. refl.	210	216	214	254	254	255	257	258
R merging	0.019	0.010	0.009	0.011	0.032	0.030	0.033	0.037
used refl. ***	399	409	409	956	787	489	501	477
R^2 ****	0.0194	0.0129	0.0135	0.0185	0.0302	0.0268	0.0304	0.0280
R^2 °	0.0216	0.0142	0.0145	0.0194	0.0312	0.0293	0.0309	0.0297
wR^2 ****	0.0314	0.0242	0.0221	0.0242	0.0410	0.0346	0.0361	0.0330
wR^2 °	0.0374	0.0277	0.0248	0.0253	0.0427	0.0368	0.0376	0.0354

* collection of reference data at room temperature without furnace or cryostat.

** data collection at room temperature with the crystal inside the mirror furnace.

*** unaveraged reflections used in the refinement are in the range $0.83 < [I^2(\text{obs})/I^2(\text{calc})] < 1.20$ in order to exclude weak unobserved reflections.

**** including third- and fourth-order coefficients of displacement tensors.

\clubsuit 2 θ < 40°; \spadesuit 2 θ > 40°.

on a four-circle Huber diffractometer. The temperature stability and accuracy are estimated to be within ± 1 K of the nominal values.

The required high temperatures were attained by a prototype mirror furnace designed by one of us (RKM), and carefully calibrated for this experiment. The furnace is composed of an evacuated gold-coated aluminum ellipsoid. The radiation emitted by a halogen lamp located on one focus is totally reflected to the other focus, where the crystal is located and supported by a thin ceramic pole. The crystal and the Pt–Rh thermocouple are actually surrounded by a spherical Ti chamber of 1.5 cm in diameter, and the space between the crystal and the Ti wall is filled by alumina powder. The materials around the crystals were used to reduce the temperature gradients in the crystals due to heat flow along the ceramic holder. The temperature stability during data collection was within ± 2 K, and the maximum gradient across the crystal at the highest temperature was about 15 K. Details of the collection of experimental data are listed in Table 1. Analytical absorption corrections were performed on the diffraction data.

Structure refinement

The structure refinement at different temperatures was carried out using a locally modified version of the UPALS system of computer programs (Lundgren 1982), that allows testing of different extinction models and application of the higher cumulants analysis of the atomic displacement parameters. Two sets of refinements were carried out in parallel for each data-set. One structure refinement used the integrated intensities extracted with the conventional integration techniques, whereas the other structure refinement used the intensities extracted by an especially developed profile-fitting technique, which includes proper treatment of background, exclusion of diffraction effects from multiple scattering, and correction for truncation of peak tail (Pavese & Artioli 1996). The two refinements gave rather similar structural results, because of the good quality of the collected profiles even at the highest temperatures; by employing the profile-fitting method, it was possible to retrieve a larger number of weak reflections partly overlapped by the powder-diffraction lines of the furnace materials (aluminum, titanium, corundum). The latter refinement therefore includes a larger number of observable data, and the estimated standard deviations of the refined parameters are reduced by a factor in the range 20–25%. The following discussion is based on the results of refinements carried out on the profile-fitted intensities. The agreement indices for merging of equivalent reflections are shown in Table 1, and allow an evaluation of the internal consistency of each data-set. The unmerged reflection data-sets were actually used in the least-squares fitting procedures, since residual absorption effects, due to conditioning chambers and depending on the collection angles, led to equivalent reflections that were not fully comparable. Moreover, the use, in the refinements, of a cutoff based on F_o/F_c agreement, warranted the exclusion

TABLE 2. RESULTS OF THE STRUCTURE REFINEMENTS OF PYROPE¹

T (K)	30	100	293*	295*	295**	773	973	1173
Al (0,0,0) ($\beta_{11} = \beta_{22} = \beta_{33}$; $\beta_{12} = \beta_{13} = \beta_{23}$)								
β_{11}	0.42(3)	0.34(2)	0.61(2)	0.53(1)	0.66(3)	1.35(4)	1.64(4)	1.95(4)
β_{12}	0.10(4)	0.09(3)	0.06(2)	0.00(1)	-0.07(4)	-0.07(5)	-0.03(5)	0.01(5)
Si (3/8,0,1/4) ($\beta_{22} = \beta_{33}$; $\beta_{12} = \beta_{13} = \beta_{23} = 0$)								
β_{11}	0.45(5)	0.34(4)	0.58(3)	0.47(2)	0.51(6)	1.05(7)	1.36(7)	1.55(8)
β_{22}	0.43(3)	0.39(2)	0.63(2)	0.47(1)	0.39(4)	1.14(4)	1.36(4)	1.68(5)
Mg (0,1/4,1/8) ($\beta_{11} = \beta_{22}$; $\beta_{13} = \beta_{23} = 0$)								
β_{11}	0.70(3)	0.84(2)	1.67(2)	1.59(1)	1.57(3)	3.77(5)	4.60(5)	5.52(6)
β_{22}	0.45(4)	0.38(3)	0.78(3)	0.66(2)	0.61(5)	1.71(6)	2.16(7)	2.56(8)
β_{12}	0.06(3)	0.16(2)	0.35(2)	0.44(1)	0.22(4)	0.93(6)	1.02(7)	1.20(8)
O								
x	0.03331(9)	0.03306(6)	0.03329(3)	0.03330(7)	0.03354(9)	0.03363(9)	0.03355(9)	0.03355(9)
y	0.05076(9)	0.05031(6)	0.05016(4)	0.05026(8)	0.04935(9)	0.04909(9)	0.04853(9)	0.04853(9)
z	0.6531(1)	0.65323(7)	0.65345(8)	0.65345(8)	0.65362(9)	0.65362(9)	0.65376(9)	0.65376(9)
β_{11}	0.58(3)	0.55(2)	0.91(2)	0.809(9)	0.79(2)	1.88(3)	2.26(3)	2.66(3)
β_{22}	0.58(3)	0.61(2)	1.03(2)	0.942(9)	0.89(2)	2.23(3)	2.76(3)	3.21(3)
β_{33}	0.52(3)	0.44(2)	0.72(2)	0.62(1)	0.68(3)	1.46(3)	1.74(3)	2.10(3)
β_{12}	0.03(1)	0.05(1)	0.11(1)	0.115(6)	0.06(2)	0.27(2)	0.34(2)	0.36(3)
β_{13}	-0.02(2)	-0.06(1)	-0.14(1)	-0.160(6)	-0.19(2)	-0.44(2)	-0.54(2)	-0.67(2)
β_{23}	0.00(2)	-0.02(1)	-0.03(1)	-0.036(6)	-0.05(2)	-0.01(2)	0.00(2)	0.03(3)

* collection of reference data at room temperature without furnace or cryostat.

** data collection at room temperature with the crystal inside the mirror furnace.

¹ atomic displacement parameters are multiplied by 10^3 .

of those reflections found to be biased, as stated above.

Among the tested models for correction of the extinction effects in the Becker & Coppens (1974) formalism; the isotropic correction for a type-I crystal with a Lorentzian mosaic-spread distribution was found to yield the best results. Intensity correction-factors were in the range 1.00–1.15, showing a rather moderate extinction effect, and the root-mean-squares mosaic spread was found to be limited to the narrow range 43–92 seconds over the whole temperature interval.

In the final refinement cycles, the following parameters were simultaneously varied: the free atomic coordinates, one scale factor, one isotropic extinction coefficient, and the second-, third- and fourth-rank tensor coefficients of atomic displacement parameters for all atoms. The higher-order tensor coefficients obtained from the Gram–Charlier series expansion of the probability density were employed, as this type of analysis is universally considered the best available treatment of anharmonic dynamic effects (Kuhs 1988). Refined structural parameters are listed in Table 2.

The occupancy of the dodecahedral site was treated as $\text{Mg}_{0.92}\text{Fe}_{0.05}\text{Ca}_{0.03}$, following the results of the chemical analysis. Indeed, no significant difference in the atomic displacement parameters of the refined site was noted by the introduction of the small amount of Fe and Ca in the Mg position. Among the refined coefficients for the Gram–Charlier expansion of order above two, the γ_{113} , δ_{1111} , δ_{3333} , and δ_{1133} coefficients of Mg, the δ_{1222} coefficient of Al, the γ_{123} , δ_{2222} , and δ_{2223} coefficients of

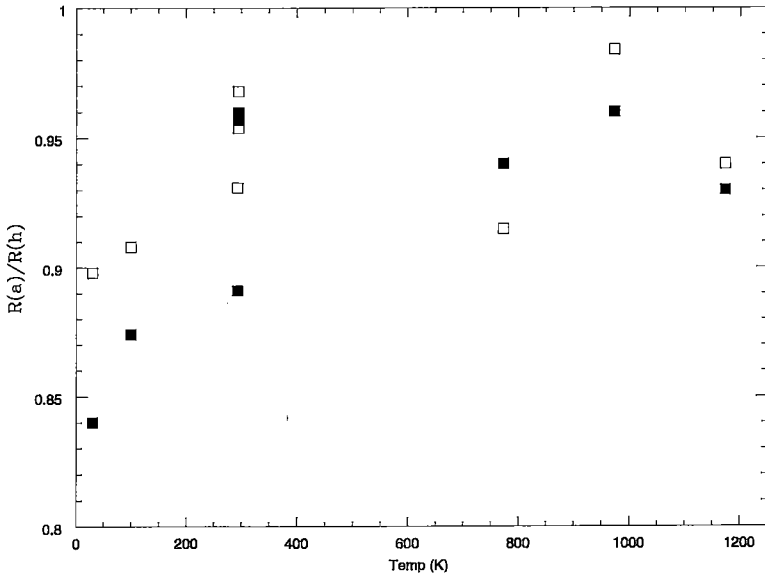


FIG. 1. Ratio of the figures of merit for the structure refinements performed using third-order (γ_{ijk}) and fourth-order (δ_{ijkl}) tensor coefficients (R_a) and second-order (β_{ij}) tensor coefficients only (R_h). The dramatic improvement of the agreement factors by the use of anharmonic thermal tensors is evident even at low temperature. Open squares (\square) refer to RF^2 factors, and solid squares (\blacksquare) refer to wRF^2 factors.

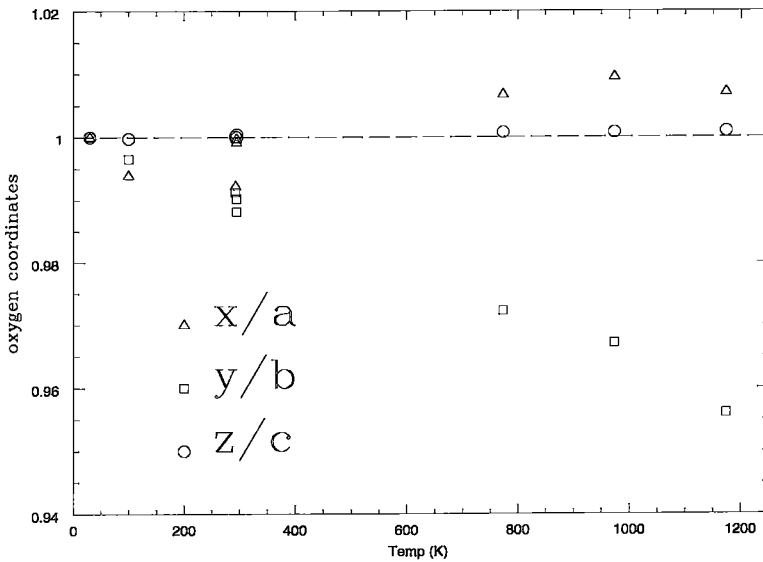


FIG. 2. Variation of the fractional coordinates of oxygen with temperature in pyrope.

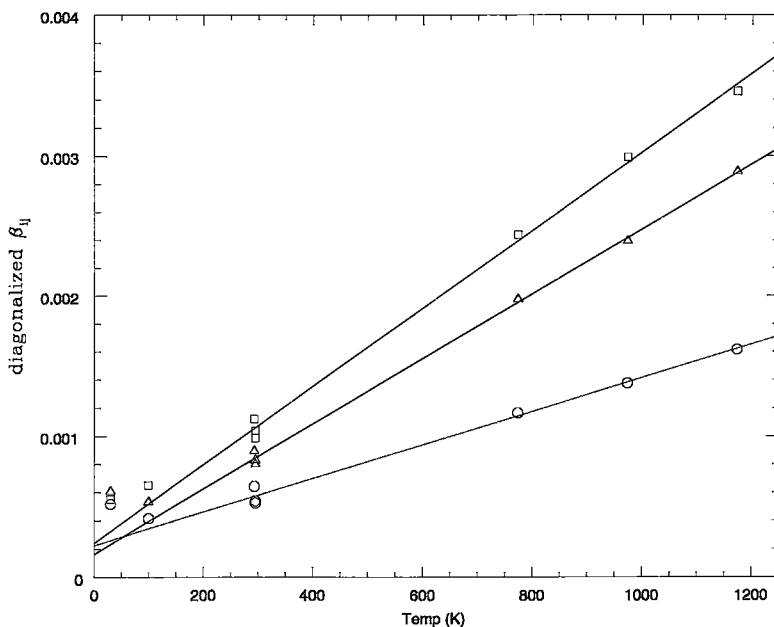


FIG. 3. Temperature dependence of the components of the diagonalized tensor of second rank of the atomic displacement of oxygen in pyrope. The lines have been obtained by least-squares fits of the components above 250 K.

Si, and the γ_{111} , γ_{222} , γ_{333} , δ_{1122} and δ_{2233} coefficients of O were different from zero at the 2–3 σ confidence level. Table 1 and Figure 1 show the reduction in the figures of merit due to the introduction of coefficients of order three and four for the Gram–Charlier expansion. It is surprising to note that there is a significant improvement in the agreement indices at low temperature, whereas it is normally assumed that anharmonic components become important only at high temperature.

RESULTS AND DISCUSSION

The geometrical interpretation of the overall response of the pyrope structure to temperature, as deduced by the present neutron-diffraction study, is rather similar to the one discussed in the previous X-ray study (Pavese *et al.* 1995); it will not be treated here in detail. However, it is important to recall that the only variable coordinates during the refinement are those of the oxygen atom, the coordinates of the other atoms being fixed by site-symmetry constraints. In Figure 2, the relative shifts in the fractional coordinates of the oxygen atom with temperature are shown: it is evident that the z coordinate is essentially fixed over the whole range of temperature, the x coordinate shows a small fluctuation only in the high-temperature range, and most of the geometrical re-arrangement in the structure is caused by the continuous and linear decrease of the y coordinate with temperature. The shift along y is directly related to the rotation of the Si-centered tetrahedron, and to the volume

increase of the Mg-centered dodecahedron (Born & Zemann 1964, Meagher 1975, Armbruster *et al.* 1992, Pavese *et al.* 1995).

The focus of the present study is to characterize features of the atomic displacements in the pyrope structure by neutron diffraction, in order to determine the nature of the structural disorder within the limits of accuracy inherent to diffraction methods. The quality of the data collected for the present study is very high, and the satisfactory overlap of the refined parameters for the experiments performed at room temperature, using different experimental setups and temperature chambers, demonstrates the excellent reproducibility of the collection and data-treatment procedures.

Diffraction data can give hints of subtle static disorder effects (*i.e.*, subsite split-atom positions) in two different ways: (1) by showing a positive intercept at 0 K of the best-fit line to the high-temperature atomic displacement parameters, or (2) by showing better figures of merit for the structural refinement of split-atom models. In the present

TABLE 3. INTERCEPT AT 0 K OF THE LINEAR BEST FIT TO THE HIGH-TEMPERATURE ($T > 250$ K) COMPONENTS OF THE DIAGONALIZED DISPLACEMENT-TENSORS OF OXYGEN AND MAGNESIUM ATOMS IN PYROPE

oxygen β'_{11}	0.00016(3)	magnesium β'_{11}	0.00025(6)
oxygen β'_{22}	0.00024(4)	magnesium β'_{22}	0.00035(8)
oxygen β'_{33}	0.00022(3)	magnesium β'_{33}	0.00005(4)

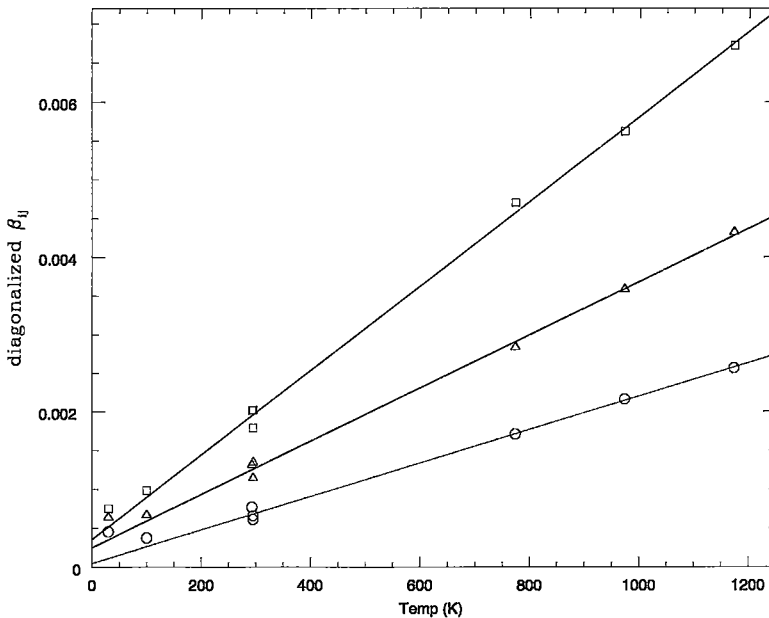


FIG. 4. Temperature dependence of the components of the diagonalized tensor of second rank of the atomic displacement of magnesium in pyrope. The lines have been obtained by least-squares fits of the components above 250 K.

case, the linear interpolation of the components of the diagonalized second-order displacement tensor (β'_{ij}) above 293 K shows a very small positive intercept at 0 K for the three principal components of the oxygen tensor (Fig. 3) and for the two components of the magnesium tensor lying in the crystallographic plane (001) (β'_{11} and β'_{22} ; Fig. 4). Intercept values are reported in Table 3. The values of the intercept are significant at the 4σ confidence level for magnesium, and at the $4-7\sigma$ confidence level for oxygen. Although these values are rather small straight-forward interpretation of the data would allow for "static" disorder in both sites. It should be pointed out, also, that based on the level of confidence, disorder on the oxygen site is more likely than on the magnesium site. This is at variance with the conclusions reached on the basis of the cited simulations of lattice dynamics, which invariably show abnormally low calculated atomic displacement parameters only on the magnesium site. Furthermore, the positive intercept on two of the magnesium tensor components indicates that if statistical disorder is present, then there are two possible subsite models for the magnesium (24c) position at (0, 1/4, 1/8): (1) two magnesium sites displaced along the diad axis along the [110] direction, or (2) four magnesium sites displaced from both diad axes on the (001) crystallographic plane. This latter model is the one postulated by Pilati *et al.* (1996). Both models were tested with our data-set collected at 30 K, by fixing a minimum distance of 0.5 Å between the statistically occupied sites on the diad or on the plane.

No significant improvement was obtained in the figures of merit associated with the refinement in both cases, with respect to the figures of merit obtained with the one-site model, and reported in Table 1. Tentative refinement of a two-atom model for the oxygen position also resulted in refinement instability and divergence.

Therefore, we conclude that the static disorder models involving several magnesium sites are not supported by the diffraction data within experimental resolution. Furthermore, the small positive intercept at 0 K, obtained by extrapolation of high-temperature components of the displacement harmonic tensor, although statistically significant up to 7σ , is not likely to be attributable to static disorder. These conclusions agree well with those obtained from single-crystal X-ray diffraction (Pavese *et al.* 1995), and provide a robust confirmation of the validity of conventional methods, where proper treatment of the data are used.

The diagonalized components of the second-order tensors at low temperature (30 and 100 K; Figs. 3, 4) are much larger than expected from the linear regression derived from the high-temperature data: this is a clear indication of the presence of the zero-point energy contribution. The contribution of the zero-point motion to the room-temperature displacement parameters, as evaluated from our 30 K data, is in the range 40–70%, and it is in agreement with previous experimental measurements on silicates [albite: Smith *et al.* (1986), natrolite: Artioli *et al.* (1984)].

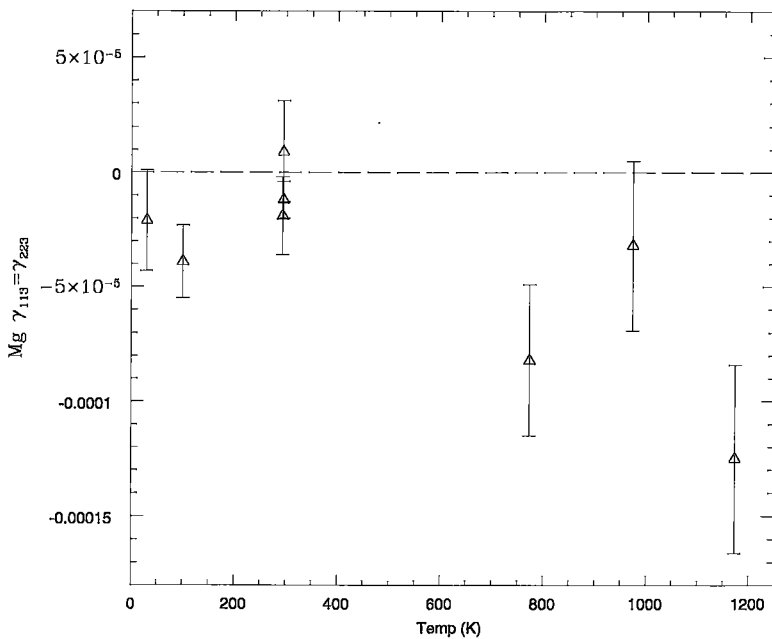


FIG. 5. Temperature dependence of the third-rank γ_{113} component of the atomic displacement tensor of the magnesium atom in pyrope.

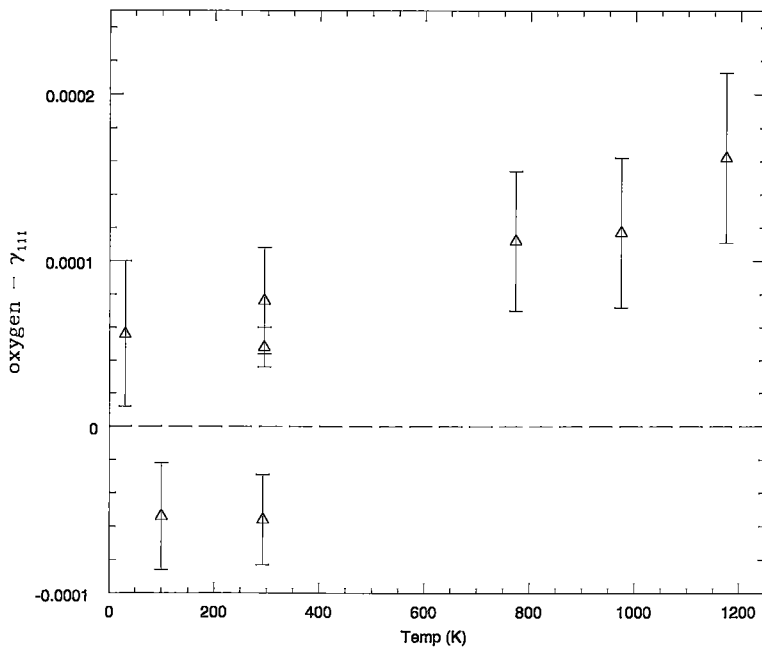


FIG. 6. Temperature dependence of the third-rank γ_{111} component of the atomic displacement tensor of the oxygen atom in pyrope.

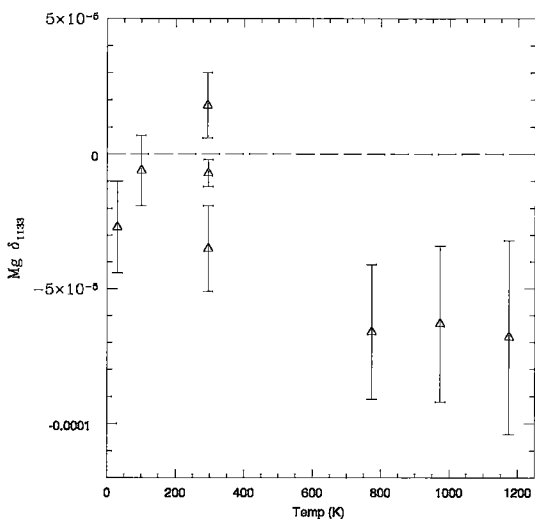


FIG. 7. Temperature dependence of the fourth-rank δ_{1133} component of the atomic displacement tensor of the magnesium atom in pyrope.

Neutron-diffraction data are also the main unequivocal experimental proof pointing to the presence of anharmonic vibrational effects in crystal structures. Since neutron data are devoid of scattering effects due to the distribution of electron density, the presence of non-zero coefficients in the refinement of higher-order cumulants of atomic displacement parameters from neutron-diffraction data is commonly taken as evidence of the presence of anharmonic contribution to atomic thermal vibration. Although anharmonic effects are often neglected in crystallographic studies of mineral structures, it is likely that their role in determining the physical and thermodynamic properties of minerals is more important than generally believed. In fact, the structure of several minerals studied in detail at high temperature [*e.g.*, anorthite: Ghose *et al.* (1993), sodalite: McMullan *et al.* (1996)] shows the clear presence of anharmonic contributions to atomic thermal vibrations.

In pyrope, the refined coefficients of the third-rank (γ_{ijk}) and fourth-rank (δ_{ijkl}) tensors are surprisingly small for all atoms in the whole range of explored temperatures. Only a few coefficients of the third-rank tensor are systematically significant at high temperature, and show a consistent trend in all data-sets above 700 K, namely the γ_{113} coefficient of Mg (Fig. 5) and the γ_{111} coefficient of O (Fig. 6). Although significant at the 3σ confidence level, the trend of these non-zero coefficients is a plausible indication that anharmonic components contribute to the thermal energy of magnesium and oxygen atoms in the high-temperature range. This is in agreement with the non-zero γ_{113} component of Mg found by the previous X-ray analysis (Pavese *et al.* 1995). The fourth-order δ_{1133} coefficient of Mg also shows the same trend at high temperature (Fig. 7).

Several of the refined high-order coefficients of the oxygen atom present a very unusual behavior: they are invariably negligible within errors in the room-temperature range, whereas they seem to be non-zero at low temperature (δ_{1133} : Fig. 8), or at low and high temperature (γ_{222} and γ_{333} : Fig. 9). The γ_{222} and γ_{333} coefficients in particular present an antithetic dependence in temperature, with a change in sign between the low- and high-temperature regions. The behavior of the γ -expansion terms could be related to the positional shift of the oxygen atom discussed above: the correlation between the shift in the x coordinate (Fig. 2) and the increase in the γ_{111} coefficient (Fig. 6) is particularly striking. Besides the change in sign, the presence of non-zero components at low temperature is especially puzzling, since in this temperature region the anharmonic contribution should in principle be absent or minimal. The presence of the non-zero high-order parameters on the oxygen atom produce a substantial improvement in the overall figure of merit (Fig. 1) of the low-temperature refinements.

It is of course unreasonable to expect significant anharmonic vibrations in the low-temperature range, especially in a structure that shows very little anharmonic contribution even at high temperature, as discussed above. It is also very unlikely that these coefficients are indicative of multiple-site positions on the oxygen site, as the exhaustive analysis of the structure presented here fails to indicate compelling evidence of site disorder on the oxygen position: (1) the 0 K intercepts shown in Figure 3 are marginally significant, as discussed above, (2) refinement of multiple positions at the oxygen site could not converge to a stable crystal-chemical model and, finally, (3) the shape of the atomic displacement ellipsoid corresponding to the

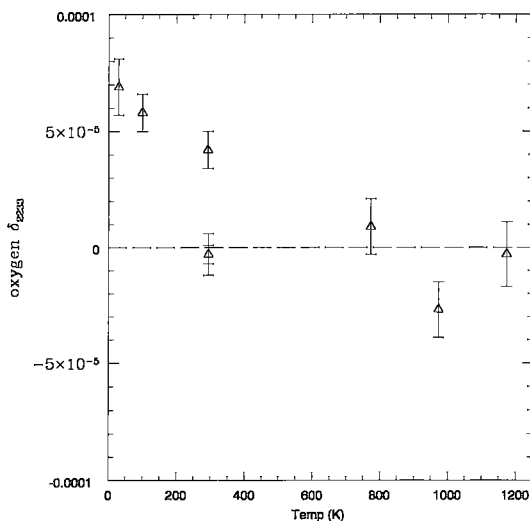


FIG. 8. Temperature dependence of the fourth-rank δ_{2233} component of the atomic displacement tensor of the oxygen atom in pyrope.

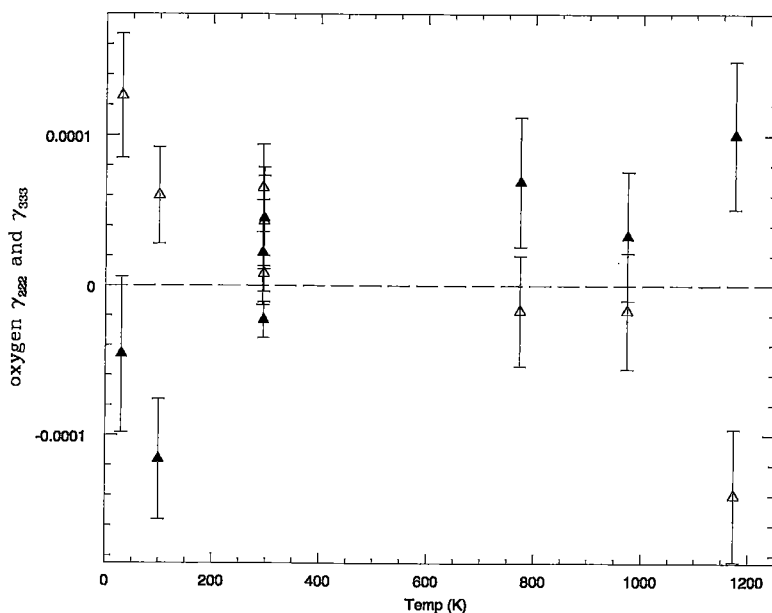


FIG. 9. Temperature dependence of the third-rank γ_{222} and γ_{333} components (open and closed triangles, respectively) of the atomic displacement tensor of the oxygen atom in pyrope.

second-rank tensor at 30 K is nearly isotropic, with very similar mean-square-displacement axial components ($\langle u^2_{11} \rangle = 0.0040 \text{ \AA}^2$, $\langle u^2_{22} \rangle = 0.0037 \text{ \AA}^2$, $\langle u^2_{33} \rangle = 0.0034 \text{ \AA}^2$), indicating that the presence of multiple positions being averaged by the refined one-atom oxygen site is most unlikely.

CONCLUSIONS

The present study of the structure of pyrope-rich garnet using single-crystal neutron-diffraction data over a wide range of temperature (30–1173 K) complements a previous study performed by single-crystal X-ray analysis (Pavese *et al.* 1995). We believe that these two investigations, carried out with state-of-the-art instrumentation and data-processing procedures, explore the limits of the information to be gained on pyrope by diffraction techniques at the present time.

These studies clearly indicate that an anharmonic contribution to the thermal vibration of the Mg and O sites is present above 700 K. The anharmonic effect is, however, very weak, and certainly much lower than expected, especially for the Mg cation, which is a relatively small ion exhibiting a large harmonic anisotropic motion inside the dodecahedral cavity.

The diffraction data fail to detect any evidence of subsite disorder on the magnesium or on the oxygen positions. In fact, in addition to other indirect evidence, any attempt to refine split-atom models has not been supported by the low-temperature neutron-diffraction data-sets.

The puzzling presence of non-zero coefficients of the high-order tensors of atomic displacement on the oxygen site at low temperature, not directly related to anharmonic motion or multiple crystallographic sites, is documented. The effect may be related to the previously reported anomalies in the low-temperature heat capacity of pyrope, and to the failure to correctly reproduce the atomic displacement parameters by simulations of lattice dynamics. These features may be due to the presence of local defects or short-range order, not detected by volume-sampling diffraction methods.

ACKNOWLEDGEMENTS

GA and AP thank Italian MURST and CNR, and KS thanks the Swedish NFR for financial support. The neutron-diffraction study at Brookhaven National Laboratory was carried out under contract DE-AC02-76CH00016 with the U.S. Department of Energy and supported by its Office of Basic Energy Sciences. Prof. G. Chiari kindly supplied the Dora Maira pyrope megablasts for this study. Dr. L. Lutterotti helped in the texture analysis. Electron-probe micro-analyses were kindly performed by Prof. R. Rinaldi. H. Rundlof helped during neutron-diffraction measurements at the Studsvik Neutron Research Laboratory. C. Koehler helped during the setup of the mirror furnace at the Brookhaven National Laboratory. We thank referees Thomas Armbruster and Roberta Oberti for their pertinent comments, and Associate Editor Pier Francesco Zanazzi, who handled the manuscript.

REFERENCES

- AMISANO CANESI, A., CHIARI, G., LUTTEROTTI, L. & SCARDI, P. (1994): Texture characterization of a porphyroblastic pyrope. *Mat. Sci. Forum* **166-169**, 731-736.
- ARMBRUSTER, T. & GEIGER, C.A. (1993): Andradite crystal chemistry, dynamic X-site disorder and structural strain in silicate garnets. *Eur. J. Mineral.* **5**, 59-71.
- _____, _____ & LAGER, G.A. (1992): Single crystal X-ray structure study of synthetic pyrope almandine garnets at 100 and 293 K. *Am. Mineral.* **77**, 512-521.
- ARTIOLI, G., SMITH, J.V. & KVICK, Å. (1984): Neutron diffraction study of natrolite, $\text{Na}_2\text{Al}_2\text{Si}_3\text{O}_{10}\cdot 2\text{H}_2\text{O}$, at 20 K. *Acta Crystallogr.* **C40**, 1658-1662.
- BECKER P.J. & COPPENS, P. (1974): Extinction within the limit of validity of the Darwin transfer equations. I. General formalism for primary and secondary extinction and their application to spherical crystals. *Acta Crystallogr.* **A30**, 129-147.
- BERMAN, R.G. (1990): Mixing properties of Ca-Mg-Fe-Mn garnets. *Am. Mineral.* **75**, 328-344
- BORN, L. & ZEMANN, J. (1964): Abstandsberechnungen und gitterenergetische Berechnungen an Granaten. *Beitr. Mineral. Petrol.* **10**, 2-23.
- CHOPIN, C. (1984): Coesite and pure pyrope in high-grade blueschists of the Western Alps: a first record and some consequences. *Contrib. Mineral. Petrol.* **86**, 107-118.
- CRESSEY, G. (1981): Entropies and enthalpies of aluminosilicate garnets. *Contrib. Mineral. Petrol.* **76**, 413-419.
- GANGULY, J., CHENG, W. & O'NEIL, H.ST. (1993): Syntheses, volume and structural changes of garnets in the pyrope-grossular join: implication for stability and mixing properties. *Am. Mineral.* **78**, 583-593.
- GEIGER, C.A., MERWIN, L. & SEBALD, A. (1992): Structural investigation of pyrope garnet using temperature-dependent FTIR and ^{29}Si and ^{27}Al MAS NMR spectroscopy. *Am. Mineral.* **77**, 713-717.
- _____, NEWTON, R.C. & KLEPPA, O.J. (1987): Enthalpy of mixing of synthetic almandine-grossular and almandine-pyrope garnets from high temperature solution calorimetry. *Geochim. Cosmochim. Acta* **51**, 1755-1763.
- GHOSE, S., McMULLAN, R.K. & WEBER, H.-P. (1993): Neutron diffraction studies of the $P1 \rightarrow I1$ transition in anorthite, $\text{CaAl}_2\text{Si}_2\text{O}_8$, and the crystal structure of the body-centered phase at 514 K. *Z. Kristallogr.* **204**, 215-237.
- GIBBS, G.V. & SMITH, J.V. (1965): Refinement of the crystal structure of synthetic pyrope. *Am. Mineral.* **50**, 2023-2039.
- HASELTON, H.T. & WESTRUM, E.F. (1980): Low temperature heat capacities of synthetic pyrope, grossular and pyrope₆₀grossular₄₀. *Geochim. Cosmochim. Acta* **44**, 701-709.
- HOFMEISTER, A.M. & CHOPELAS, A. (1991): Thermodynamic properties of pyrope and grossular from vibrational spectroscopy. *Am. Mineral.* **76**, 880-891.
- KIEFFER, S.W. (1980): Thermodynamics and lattice vibrations of minerals. 4. Application to chain and sheet silicates and orthosilicates. *Rev. Geophys. Space Phys.* **18**, 862-886.
- KOZIOL, A.M. & BOHLEN, S.R. (1992): Solution properties of almandine-pyrope garnets as determined by phase equilibrium experiments. *Am. Mineral.* **77**, 765-773.
- KUHS, W.F. (1988): The anharmonic temperature factor in crystallographic structure analysis. *Aust. J. Phys.* **41**, 369-382.
- LUNDGREN, J.O. (1982): Report N. UUIC-913-4-05. University of Uppsala, Uppsala, Sweden.
- McMULLAN, R.K., GHOSE, S., HAGA, N. & SCHOMAKER, V. (1996): Sodalite, $\text{Na}_4\text{Si}_3\text{Al}_3\text{O}_{12}\text{Cl}$: structure and ionic mobility at high temperature by neutron diffraction. *Acta Crystallogr.* **B52**, 616-627.
- MEAGHER, E.P. (1975): The crystal structure of pyrope and grossularite at elevated temperatures. *Am. Mineral.* **60**, 218-228.
- PATEL, A., PRICE, G.D. & MENDELSSOHN, M.J. (1991): A computer simulation approach to modelling the structure, thermodynamics and oxygen isotope equilibria of silicates. *Phys. Chem. Minerals* **17**, 690-699.
- PAVESE, A. & ARTIOLI, G. (1996): Profile-fitting integration of single crystal diffraction data. *Acta Crystallogr.* **A52**, 890-897.
- _____, _____ & PRENCIPE, M. (1995): X-ray single-crystal diffraction study of pyrope in the temperature range 30-973 K. *Am. Mineral.* **80**, 457-464.
- PILATI, T., DEMARTIN, F. & GRAMACCIOLI, C.M. (1996): Atomic displacement parameters for garnets: a lattice-dynamical evaluation. *Acta Crystallogr.* **B52**, 239-250.
- QUARTIERI, S., CHABOY, J., MERLI, M., OBERTI, R. & UNGARETTI, L. (1995): Local structural environment of calcium in garnets: a combined structure-refinement and XANES investigation. *Phys. Chem. Minerals* **22**, 159-169.
- SAWADA, H. (1993): The crystal structure of garnets. I. The residual electron density distribution in pyrope. *Z. Kristallogr.* **203**, 41-48.
- SCHERTL, H.P., SCHREYER, W. & CHOPIN, C. (1991): The pyrope-coesite rocks and their country rocks at Parigi, Dora Maira Massif, Western Alps: detailed petrography, mineral chemistry, and metamorphic evolution. *Contrib. Mineral. Petrol.* **108**, 1-21.
- SMITH, J., ARTIOLI, G. & KVICK, Å. (1986): Low albite, $\text{NaAlSi}_3\text{O}_8$: neutron diffraction study of crystal structure at 13 K. *Am. Mineral.* **71**, 727-733.

- UNGARETTI, L., LEONA, M., MERLI, M. & OBERTI, R. (1995): Non-ideal solid-solution in garnet: crystal structure evidence and modelling. *Eur. J. Mineral.* **7**, 1299-1312.
- WINKLER, B., DOVE, M.T. & LESLIE, M. (1991): Static lattice energy minimization and lattice dynamics calculations on aluminosilicate minerals. *Am. Mineral.* **76**, 313-331.
- ZEMANN, A. & ZEMANN, J. (1961): Verfeinerung der Kristallstruktur von synthetischen Pyrop $Mg_3Al_2(SiO_4)_3$. *Acta Crystallogr.* **14**, 835-837.
- ZEMANN, J. (1962): Zur Kristallchemie der Granate. *Beitr. Mineral. Petrol.* **8**, 180-188.
- Received January 19, 1997, revised manuscript accepted July 15, 1997.*